

# Long wavelength InAs<sub>0.05</sub>Sb<sub>0.95</sub> photodiodes grown by melt epitaxy

Y. Z. GAO<sup>a,\*</sup>, X. Y. GONG<sup>a</sup>, T. MAKINO<sup>b</sup>, H. KAN<sup>b</sup>, T. KOYAMA<sup>c</sup>, Y. HAYAKAWA<sup>c</sup>

<sup>a</sup>College of Electronics and Information Engineering, Tongji University, Shanghai 201804, China

<sup>b</sup>Central Research Laboratory, Hamamatsu Photonics K. K., Hamakita, Shizuoka 434-8601, Japan

<sup>c</sup>Research Institute of Electronics, Shizuoka University, Johoku 3-5-1, Hamamatsu, Shizuoka 432-8011, Japan

InAs<sub>0.05</sub>Sb<sub>0.95</sub> thick epilayers were grown on InAs substrates by melt epitaxy (ME). Long wavelength photodiodes made from the thick epilayers were obtained operating at 77 K. Homojunctions were formed on n-InAs<sub>0.05</sub>Sb<sub>0.95</sub> wafers by zinc diffusion. Current-voltage characteristics of p-n junctions were measured at 50 K, 77 K and 100 K respectively. The dark current density is  $2.4 \times 10^{-4}$  A/cm<sup>2</sup> under -10 mV bias at 77 K. Spectral photoresponse of the devices showed that 50% cutoff wavelength is 8  $\mu$ m, and 20% cutoff wavelength is 9  $\mu$ m. It indicates promising prospect for infrared (IR) detection.

(Received January 14, 2019; accepted October 9, 2019)

**Keywords:** Long wavelength, InAsSb, Melt epitaxy, Spectral photoresponse

## 1. Introduction

IR photon detectors with long wavelength have many important applications, such as remote sensing, meteorological satellite, resources detection, measuring temperature, and medical diagnosis. HgCdTe detector is the currently dominant system in the wavelength range of 8-12  $\mu$ m. However, it suffers from chemical instability and nonuniformity owing to the high Hg vapor pressure during its growth. This problem becomes more obvious as the temperature raising in the long wavelength range. Among III-V compounds, InAsSb ternary alloy has attractive advantages of narrow band gap, high electron and hole mobilities, low electron effective mass, good chemical stability and mechanical strength, and long performance life. Therefore it becomes a very promising material alternative to HgCdTe [1, 2]. Recently, type-II antimonide-based infrared detectors have been reported [3-8]. Long wavelength IR photodiodes with a 50% cutoff wavelength of 8  $\mu$ m grown by metalorganic chemical vapor deposition (MOCVD) have been demonstrated at 77 K [5].

In our previous papers, uncooled long wavelength InAsSb photoconductors without p-n junctions were reported [9-10]. InAsSb thick epilayers with cutoff wavelengths longer than 8  $\mu$ m were grown on InAs substrates by melt epitaxy (ME), and ME is modified liquid phase epitaxy (LPE) [11-12]. The thickness of the epilayers reached 100  $\mu$ m. This thickness effectively suppressed the affection of the lattice mismatch resulting in a low dislocation density (the order of  $10^4$  cm<sup>-2</sup>) and high crystal quality of the epilayers. However, InAsSb photodiodes with p-n junctions made from the thick

epilayers have not yet been studied. In this paper, initial InAs<sub>0.05</sub>Sb<sub>0.95</sub> photodiodes grown by ME were obtained. *I-V* characteristics and spectral photoresponse of long wavelength photodiodes were measured at 77 K.

## 2. Experimental

InAsSb epilayers were grown on (100)-oriented n-InAs substrates in a horizontal LPE growth system in high purity hydrogen ambient. The source materials were 7N Sb, In and non-doped InAs single crystals. The detailed growth process of ME has been provided in our previous paper [12]. The key point is as follows: at the growth temperature (about 500 °C), the melt is pushed to contact with the substrate, and the excess growth melt is immediately removed away from the substrate by pushing the melt holder. It is important that some melt is remained on the surface of the substrate at the growth temperature. Then the substrate was pushed under the flat part (the block) of the melt holder and cooled with a cooling rate of 0.5°C/min to obtain an epilayer. The surface of the samples has been polished to mirror smooth by Al<sub>2</sub>O<sub>3</sub> powders.

The planar structure photodiodes with p-n junctions were fabricated using InAs<sub>0.05</sub>Sb<sub>0.95</sub> samples by a conventional device process. SiN thin films with the thickness of 1000 Å were evaporated on the surface of InAsSb samples as masks for diffusion. Homojunctions were formed by diffusing Zn at 450 °C in high purity hydrogen atmosphere. Zn is p-type impurity for n-InAsSb materials. The vapor of Zn is high, and it can be easily diffused into n-samples. Therefore we employed Zn as

diffusing source. Au-Ge-Ni and Cr-Au were used as electrodes for n-side and p-side respectively. The light sensitive surface of InAsSb photodiodes is a circle with diameter of 1 mm, and the area of it is 0.00785 cm<sup>2</sup>. There are not any lens and antireflection coatings on the photodiodes.

### 3. Results and discussion

#### 3.1. X-ray diffraction curves

Fig. 1 shows X-ray diffraction (XRD) patterns of InAs/InAsSb samples measured by an X-ray diffractometer (Rigaku D/MAX-2200PC, Cu barn) at a voltage of 40 kV and a current of 40 mA.

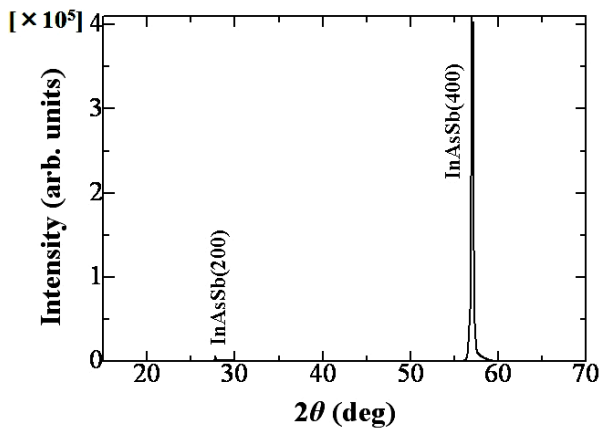


Fig. 1. X-ray diffraction curves of InAs<sub>0.05</sub>Sb<sub>0.95</sub> samples grown by ME. The lattice constant of InAs<sub>0.05</sub>Sb<sub>0.95</sub> samples is estimated to be 6.4572 Å

In Fig. 1, (400) and (200) diffraction peaks of InAsSb epilayers clearly appear, and no other crystal structures are observed. The growth direction of the epilayers agrees with the surface direction of InAs substrates, i.e. (100) orientation. This demonstrates that InAsSb epilayers are indeed single crystals. Because the thickness of the epilayers grown by ME reaches 100 μm, the diffraction peaks of InAs substrates are not observed. The full-width at half-maximum (FWHM) of InAsSb (400) diffraction peak is 176 arcsec indicating the high quality of the epilayers.

According to Bragg diffraction equation, the lattice constant  $a$  for InAs <sub>$x$</sub> Sb <sub>$1-x$</sub>  samples shown in Fig. 1 is estimated to be 6.4572 Å. Based on Vegard Law [13], the arsenic mole fraction in the epilayers can be calculated as

$$x = (a_{\text{InAsSb}} - a_{\text{InSb}}) / (a_{\text{InAs}} - a_{\text{InSb}}) \quad (1)$$

where  $x$  is the arsenic mole fraction in the epilayers. The arsenic mole fraction is calculated to be 0.05. The compositions of the epilayers were measured using

electron probe microanalysis (EPMA, JEOL JXA-8530F) at a voltage of 15 kV. The arsenic atomic fraction in the epilayers with the thickness of 100 μm measured by EPMA is 5.1%, which is consistent with that obtained by XRD measurements.

#### 3.2. Current-voltage characteristics

Fig. 2 shows the cross section of InAsSb p-n junctions observed by a Nomarski optical microscope.

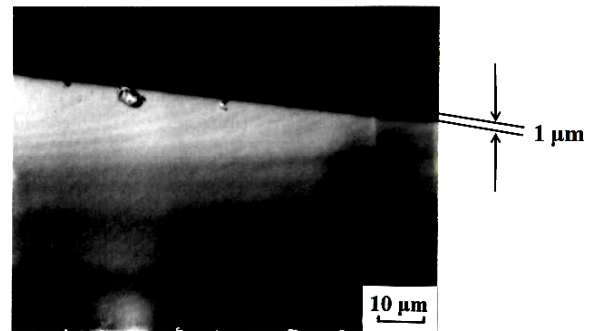


Fig. 2. Cross-sectional image of an InAs<sub>0.05</sub>Sb<sub>0.95</sub> p-n junction observed by optical microscope

As shown in Fig. 2, the black line indicates p-n junction was formed, which is flat and straight implying the good quality of the junction. The depth of p-n junction location is 1 μm.

Fig. 3 shows current-voltage characteristics of InAs<sub>0.05</sub>Sb<sub>0.95</sub> photodiodes measured by a semiconductor parameter analyzer (CHI660B) at 50 K (a), 77 K (b) and 100 K (c). The rectifying characteristics of p-n junctions are observed. The diffusion current dominates with the forward voltage rising. At a given forward bias, the diffusion current increases as the temperature increasing from 50 K to 100 K. The differential resistance at zero bias ( $R_0A$ ) is 68, 40 and 17 Ω cm<sup>2</sup> at 50 K, 77 K and 100 K respectively. It indicates that fine p-n junctions have been obtained. The dark current density is  $1.5 \times 10^{-4}$ ,  $2.4 \times 10^{-4}$  and  $5.6 \times 10^{-4}$  A/cm<sup>2</sup> under -10 mV bias at 50 K, 77 K and 100 K respectively. For reverse biased p-n junctions, the generation-recombination (G-R) current dominates the dark current at low temperatures. The depletion layer width increases with reverse bias voltage increasing. Thus the generation of carriers and reverse current raise with reverse bias raising. In Fig. 3, the reverse current based on G-R current does not saturate at 50 K, 77 K and 100 K respectively, which is larger than the saturation current owing to diffusion current. The temperature dependence of G-R current can be expressed as follows [14].

$$I_{G-R} = (qn_iAW / \tau_e) [1 - \exp(-qV/kT)] \quad (2)$$

where  $T$  is the temperature,  $q$  is the electron charge,  $n_i$  is the intrinsic carrier density,  $A$  is the area of junction,  $W$  is the width of depletion layer,  $\tau_e$  is the lifetime of electron,  $k$  is Boltzmann constant, and  $V$  is the bias voltage.  $n_i$  is related to the energy band gap of material and the temperature.

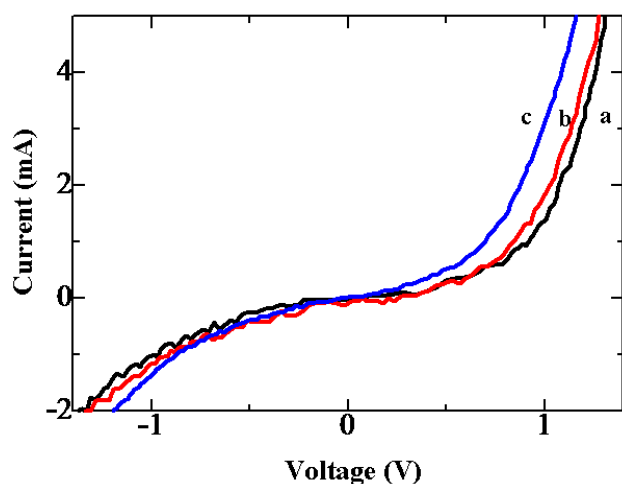


Fig. 3. Current-voltage characteristics of InAs<sub>0.05</sub>Sb<sub>0.95</sub> photodiodes at 50 K (a), 77 K (b) and 100 K (c)

### 3.3. Spectral photoresponse

Fig. 4 shows spectral photoresponse of InAs<sub>0.05</sub>Sb<sub>0.95</sub> photodiodes measured by a mid-infrared device spectroscopic characteristic measurement system with the ceramics light source at 77 K. In Fig. 4, the peak wavelength is 6.5  $\mu\text{m}$ . 50% cutoff wavelength is 8  $\mu\text{m}$ , and the corresponding energy band gap is 0.155 eV. An obvious photoresponse is observed beyond the wavelength of 8  $\mu\text{m}$ , and 20% cutoff wavelength is 9  $\mu\text{m}$ .

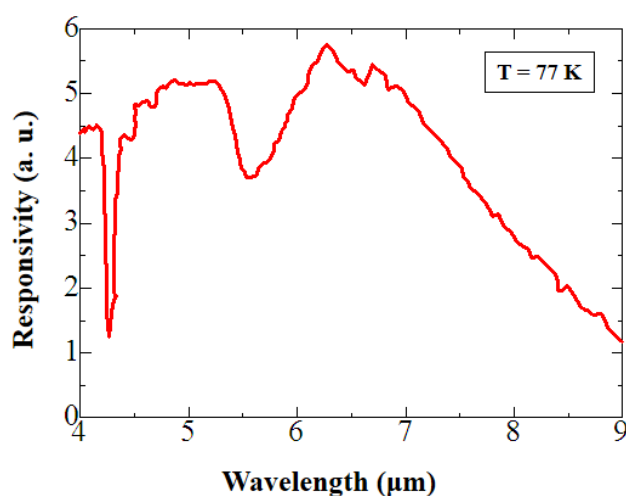


Fig. 4. Spectral photoresponse of InAs<sub>0.05</sub>Sb<sub>0.95</sub> photodiodes at 77 K

The cutoff wavelength of InSb is 5.5  $\mu\text{m}$  with the corresponding energy band gap of 0.225 eV at 77 K. It is evident that the energy band gap of InAs<sub>0.05</sub>Sb<sub>0.95</sub> is narrower than that of InSb. The band gap narrowing of InAs<sub>0.05</sub>Sb<sub>0.95</sub> materials may mainly caused by lattice contraction. The lattice constant of InAs<sub>0.05</sub>Sb<sub>0.95</sub> (6.4572  $\text{\AA}$ ) is smaller than that of InSb (6.4789  $\text{\AA}$ ). It indicates the lattice compression of InAs<sub>0.05</sub>Sb<sub>0.95</sub> crystals due to arsenic atoms combination in the lattice, i.e. arsenic atoms substitute the locations of some antimony atoms. Additionally, the non-regular arrangement of atoms in the lattice may also affect the energy band bowing for III-V mixed crystals. As shown in Fig. 4, the absorption dip at 4.3  $\mu\text{m}$  is observed in the spectral photoresponse, which is resulted from CO<sub>2</sub> absorption. The absorption dip at 5.6  $\mu\text{m}$  may be due to H<sub>2</sub>O absorption.

## 4. Conclusions

In this study, long wavelength InAsSb photodiodes operating at 77 K were fabricated. The photodiodes were based on InAs<sub>0.05</sub>Sb<sub>0.95</sub> thick epilayers on InAs substrates grown by ME. At 77 K, current-voltage characteristics and spectral photoresponse of the photodiodes were measured. 50% cutoff wavelength of InAs<sub>0.05</sub>Sb<sub>0.95</sub> is 8  $\mu\text{m}$  with the corresponding energy band gap of 0.155 eV. It indicates narrow band gap antimonide materials have been obtained.

## Acknowledgments

The authors acknowledge the financial assistance provided by the Research Funds for National Defence in China.

## References

- [1] G. Belenky, D. Donetsky, G. Kipshidze, D. Wang, L. Shterengas, W. L. Sarney, S. P. Svensson, *Appl. Phys. Lett.* **99**, 141116 (2011).
- [2] D. Lackner, M. Steger, M. L. W. Thewalt, O. J. Pitts, Y. T. Cherng, S. P. Watkins, E. Plis, S. Krishna, *J. Appl. Phys.* **111**, 034507 (2012).
- [3] E. H. Steenbergen, Y. Huang, J. -H. Ryou, L. Ouyang, J. -J. Li, D. J. Smith, R. D. Dupuis, Y. -H. Zhang, *Appl. Phys. Lett.* **99**, 071111 (2011).
- [4] Z. D. Ning, S. M. Liu, S. Luo, F. Ren, F. J. Wang, T. Yang, F. Q. Liu, Z. G. Wang, L. C. Zhao, *Appl. Surface Science* **368**, 110 (2016).
- [5] D. H. Wu, A. Dehzangi, Y. Y. Zhang, M. Razeghi, *Appl. Phys. Lett.* **112**, 241103 (2018).
- [6] D. Wu, A. Dehzangi, M. Razeghi, *Appl. Phys. Lett.* **115**, 0061102 (2019).
- [7] A. Soibel, D. Z. Ting, S. B. Rafol, A. M. Fisher, S. A. Keo, A. Khoshakhlagh, S. D. Gunapala, *Appl. Phys.*

- Lett. **114**, 161103 (2019).
- [8] J. Tong, L. Y. M. Tobing, S. Qiu, D. H. Zhang, A. G. Unil Perera, Appl. Phys. Lett. **113**, 011110 (2018).
- [9] Y. Z. Gao, X. Y. Gong, G. H. Wu, Y. B. Feng, T. Makino, H. Kan, Jpn. J. Appl. Phys. **50**, 060206 (2011).
- [10] Y. Z. Gao, X. Y. Gong, G. H. Wu, Y. B. Feng, T. Koyama, Y. Hayakawa, Optoelectron. Adv. Mat. **8**(11-12), 1115 (2014).
- [11] Y. Z. Gao, X. Y. Gong, H. Kan, M. Aoyama, T. Yamaguchi, Jpn. J. Appl. Phys. **38**, 1939 (1999).
- [12] Y. Z. Gao, H. Kan, F. S. Gao, X. Y. Gong, T. Yamaguchi, J. Cryst. Growth. **234**, 85 (2002).
- [13] A. R. Denton, N. W. Ashcroft, Phys. Rev. A. **43**, 3161 (1991).
- [14] M. Feng, L.W. Cook, M. M. Tashima, T. H. Windhorn, G. E. Strillman, Appl. Phys. Lett. **34**, 292 (1979).

---

\*Corresponding author: gaoyuzhu@tongji.edu.cn